TWENTY FIRST EUROPEAN ROTORCRAFT FORUM

Paper No. VII-4

IDENTIFICATION OF LINEAR MODELS OF THE UH-60 IN HOVER AND FORWARD FLIGHT

Jay W. Fletcher
U.S. Army Aeroflightdynamics Directorate
Aviation Research, Development and Engineering Center
Aviation and Troop Command
Ames Research Center
Moffett Field, CA
USA

August 30 - September 1, 1995
Saint-Petersburg, Russia

Paper nr.: VII.4

Identification of Linear Models of the UH-60 in Hover and Forward Flight.

J.W. Fletcher

TWENTY FIRST EUROPEAN ROTORCRAFT FORUM
August 30 - September 1, 1995 Saint-Petersburg, Russia

IDENTIFICATION OF LINEAR MODELS OF THE UH-60 IN HOVER AND FORWARD FLIGHT

Jay W. Fletcher
Aeroflightdynamics Directorate
Aviation Research and Engineering Center
U.S. Army Aviation and Troop Command
Ames Research Center
Moffett Field, CA USA

Abstract

A linear model structure applicable to identification of the UH-60 flight dynamics in hover and forward flight without rotor state data is developed. The structure of the model is determined through consideration of the important dynamic modes of the UH-60 in the frequency range of interest for flight control applications. Included are the six fuselage rigid body degrees of freedom, the rotor tip-path-plane flap and lead-lag dynamics, the main rotor RPM and induced velocity dynamics, and engine gas generator and governor dynamics. An empirical correction to the flapping equations referred to as the "aerodynamic phase lag" is included which emulates the effects of the main rotor dynamic wake on the development of flapping moments. The model structure is employed in the identification of linear models of the UH-60 from flight test data at hover and 80 kts forward flight using a frequency-response-error identification method. The models are fit to flight-identified frequency responses through the adjustment of the values of the model parameters. Systematic model structure reduction is performed to ensure that minimally parameterized models are obtained. The identified models match the flight test data well, predict the rigid body response of the UH-60 better than current generation blade element simulation models, and are accurate from approximately 0.5 to 20 rad/sec. The identified physical flapping parameters correlate well with theoretical results. The aerodynamic phase lag formulation is shown to be an effective approach to improving the prediction of the aircraft off-axis angular rate responses.

Notation

a	blade lift curve slope
a_0	blade coning angle measured from hub plane, rad
a_1	longitudinal tip-path-plane tilt, rad
b_1	lateral tip path plane tilt, rad
a_x	longintudinal body axis specific force,ft/sec^2
a_y	lateral body axis specific force, ft/sec^2
a_z	vertical body axis specific force, ft/sec^2
A_1	longitudinal swashplate angle, rad
B_1	lateral swashplate angle, rad
c	blade chord, ft
e	flapping hinge offset, ft
K_C	fuel controller anticipation gain, lbm/in-sec
K_D	fuel controller derivative gain, lbm-sec
K_I	fuel controller integral gain, lbm/sec
K_P	fuel controller proportional gain, lbm
m	aircraft mass, slugs
M_{11}	vertical induced velocity apparent mass, slugs
N	number of blades
p	body axis roll rate perturbation, rad/sec
q	body axis pitch rate perturbation, rad/sec
r	body axis yaw rate perturbation, rad/sec
Q	equivalent shaft torque perturbation, ft-lbf
R	main rotor radius, ft
u	body axis lon airspeed perturbation, ft/sec
v	body axis lat airspeed perturbation, ft/sec
w	body axis vert airspeed perturbations, ft/sec
w_f	fuel flow rate perturbation, lbm/sec
x	body longitudinal axis, positive forward
y	body lateral axis, positive right wing
z	body vertical axis, positive down
δ_{lat}	lateral cyclic control perturbation, inch
δ_{lon}	longitudinal cyclic control perturbation, inch
δ_{ped}	pedal control perturbation, inch
δ_{col}	collective control perturbation, inch
Ψ	main rotor azimuth angle, rad
ψ_a	aerodynamic phase lag, rad
τ_{w_f}	fuel flow time constant, sec
Ω	engine/rotor angular velocity, rad/sec
δ	blade mean profile drag coefficient
δ_3	pitch/flap coupling, rad
ρ	air density, slugs/ft^3
σ	main rotor solidity ratio
λ	inflow ratio
μ	advance ratio
υ	induded velocity, ft/sec
ν	non-dimensional induced velocity
γ	Lock Number
ε	e/R
M_β	blade first flapwise mass moment, slug-ft
I_β	blade second flapwise mass moment, slug-ft^2
θ	aircraft pitch Euler angle, rad
θ_0	swashplate collective pitch angle, rad
θ_{tr}	tail rotor collective pitch angle, rad
θ_t	main rotor blade twist angle, rad
ϕ	aircraft roll Euler angle, rad

Presented at the 21st European Rotorcraft Forum, Saint Petersburg, Russia, 29 August - 1 September, 1995

Introduction

Modern rotorcraft flight control system (FCS) design methods promise to yield high vehicle response bandwidth with good gust rejection. Successful achievement of these characteristics in flight depends on availability of a design model which accurately characterizes the vehicle response up to the frequency of the regressing rotor flap and lead-lag modes [1]. Unfortunately, existing, full-flight-envelope flight simulation models used by the flight controls community may not have sufficient fidelity for this application [2].

Figure 1 compares frequency responses of two state-of-the-

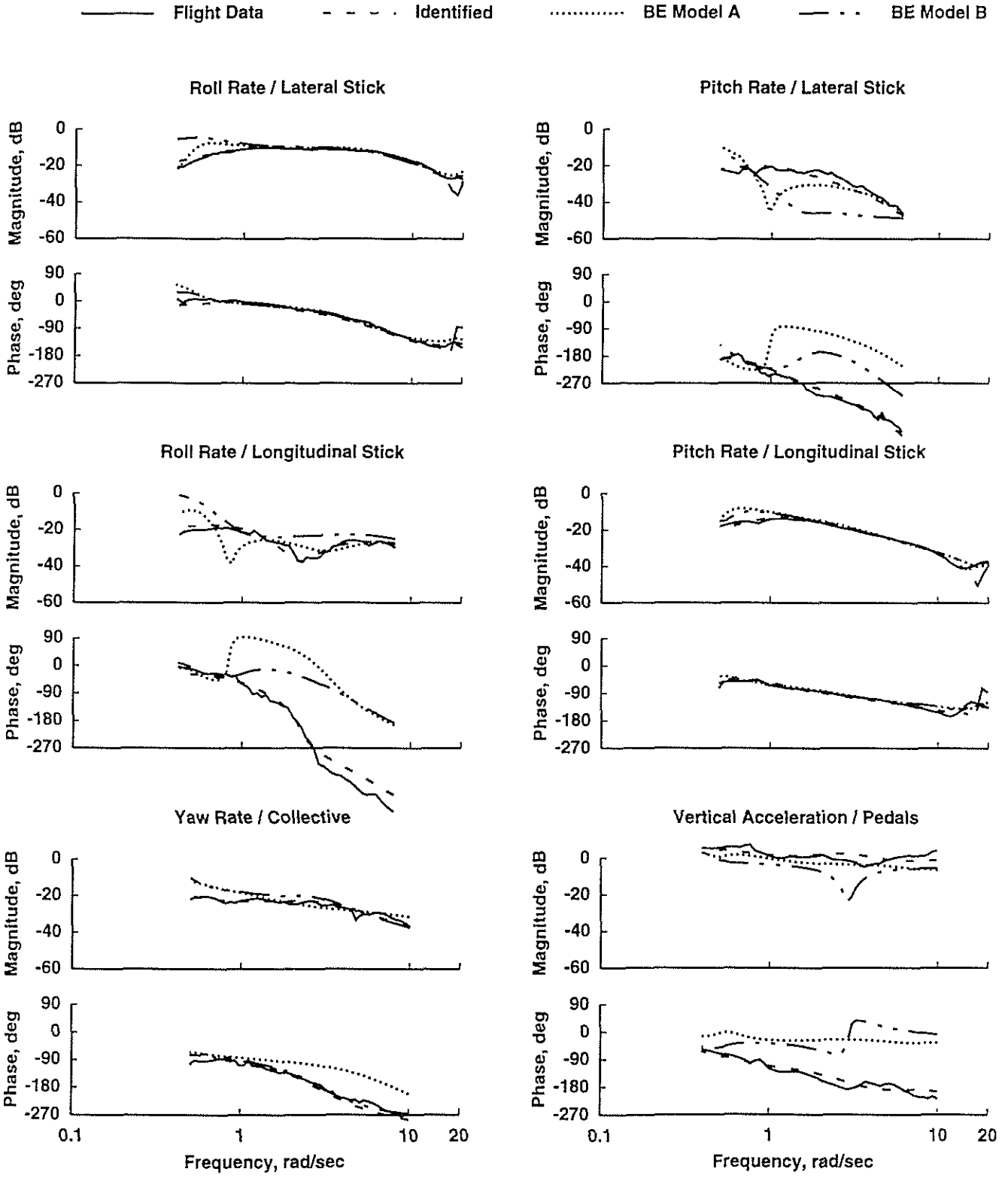

Figure 1. Comparison of Blade Element and Identification Models with Flight Test Data

art blade element flight dynamics simulation models [3, 4] of the UH-60 with frequency responses identified from hover flight test data. Each simulation model, henceforth referred to as BE Model A and BE Model B respectively, includes second-order flap and lead-lag dynamics and a three-state dynamic induced velocity model [5]. BE Model B also includes one main rotor RPM degree of freedom (DOF) and engine/governor dynamics. Both models predict the on-axis responses well to about 10 rad/sec but have deficiencies in their off-axis angular rate response prediction. The discrepancies in the off-axis are of critical significance for FCS design since they may prevent decoupling and stability margin goals from being achieved [6]. Similar off-axis modeling deficiencies have been observed in simulation models of the AH-64 [7] and BO 105 [8]. This consistent discrepancy between simulation theory and experiment has led some researchers to question some of the basic assumptions made in flight dynamical modeling of single main rotor helicopters [2].

The extraction of very accurate linear models from flight test data using system identification techniques provides an alternate source of FCS design models when such flight data are available. A linear model of the UH-60 identified from hover flight test data which includes simplified rotor flap and lead-lag dynamics is presented in ref. [9]. This model is also compared with flight test data in Figure 1. The identified model fits the on-axis angular rate responses very well up to 20 rad/sec. It also fits the pitch/roll and yaw/heave coupling responses up to the frequency limit of good coherence data at approximately 10 rad/sec.

One problem with the model is that constraints in the classical rotor flapping equations associated with dynamic coupling had to be relaxed to achieve these results. This decreases confidence in the robustness of the identification model structure. As Curtiss [2] implies, some effect is missing from the classical flapping equations and degrades fidelity in the case of the simulation models. This same effect is being compensated for by violation of constraints in the case of the identification model. A new formulation of the identification model structure is sought which will capture this effect and allow a model with correct physical constraints to be identified.

The effect in question may be the coupling of the angular degrees of freedom of the main rotor dynamic wake with the rotor flapping dynamics described by Rosen [10]. Tischler has accounted for the discrepancy of the classical flapping equations in modeling the coupling response by introducing a phasing of the aerodynamic flapping moments through an adjustment of the swashplate control phasing angle [11]. This aerodynamic phase correction was included in the UH-60 flight response identification for hover in reference [6]. In the present work this model is refined and extended to the 80 kts forward flight condition.

This paper presents the development of a generalized linear model structure applicable to identification of the UH-60 flight dynamics in hover and forward flight without rotor state data. The structure of the model was determined through consideration of the important dynamic modes in the frequency range of interest for flight control applications. Included are the six rigid body fuselage degrees of freedom as well as rotor tip-path-plane flap and lead-lag dynamics, main rotor RPM and induced velocity dynamics, and engine gas generator and governor dynamics. The aerodynamic phase lag correction to the flapping equations is included to capture the correct coupling behavior of the aircraft.

This paper also documents the application of this model structure in the identification of models of the UH-60 flight dynamics for hover and 80 kts forward flight. These models have high fidelity in the frequency range of 0.3 to 20 rad/sec and are currently being used in the design of airspeed-scheduled flight control laws for the Rotorcraft Aircrew Systems Concepts Airborne Laboratory (RASCAL) [12] UH-60 helicopter (Figure 2) at Ames Research Center [6].

Figure 2. The RASCAL UH-60 Helicopter

Identification Model Structure Formulation

The model structure formulation process consists of determining which dynamics are to be included in the model and how they are to be parameterized. This is largely determined by the required frequency range of the model and the number of dynamic states which are measured during the flight test. The effects of all of the dynamics which have significant modal responses in the desired frequency range should be included. However, it may be difficult to uniquely identify all of the dynamics if enough measurements are not available to allow the unique effects of each component of the system to be detectable in the data. In particular, it is difficult to simultaneously identify fuselage, rotor, and inflow dynamics if only fuselage measurements are available. If overparameterization occurs, some parts of the model must be fixed at theoretical values or a simplification of the dynamics must be made.

Both analytical [13,1,14] and flight [15,16] investigations have demonstrated the need to explicitly represent the dynamics in the frequency range of the regressing rotor modes in models used for the design of high bandwidth flight control systems. A major objective of this study was to determine a system identification model structure which meets this requirement and will not be overparameterized when rotor state data are not available. This objective has been achieved by coupling simplified rigid blade flapping equations valid for frequencies approaching and beyond the flap regressing mode with 6 DOF quasi-steady fuselage equations valid for frequencies below the flap regressing mode. Special care is taken not to duplicate physical effects between the stability derivatives and coefficients in the rotor flapping equations. A parasitic dipole representation of the lead-lag dynamics (one-way coupled to the aircraft on-axis angular rate response) characterizes the effects of the lead-lag

dynamics in the frequency range of interest without overparameterization.

A second objective was to determine an identification model structure which would match the off-axis flight test data without relaxing the physical constraints in the classical flapping equations. The work of Rosen, et al. in Ref. [10] on modeling unsteady aerodynamics indicates that the variation in wake geometry due to rotor pitch and roll motion has a significant effect on the development of blade aerodynamic forces and moments. This effect is not modeled in the Pitt/Peters dynamic inflow theory [5]. Rosen and his colleagues developed a complex model that accounts for the full coupling between the rotor dynamics and the wake and shows excellent correlation of rotorcraft cross-coupling in hover for both the AH-64 and UH-60 helicopters. Recent results from an identification study [11] using wind tunnel data from a full-scale shaft-fixed test of a bearingless main rotor indicate that the cross-coupling prediction of the classical flapping equations with three-state dynamic inflow could be significantly improved by adjusting the swashplate control phasing. These results were later extended to the shaft-free case of the UH-60 in hover in reference [6] by replacing the swashplate control phase angle shift by a rotor blade aerodynamic phase lag, ψ_a. The hover results are herein refined and extended to the 80 kts forward flight case as well.

Previous theoretical [17] and experimental [4,9] studies have shown that the main rotor RPM/engine/governor dynamics of the UH-60 couple significantly into the overall yaw/heave response of the aircraft in hover. In addition, the main rotor induced velocity dynamics have a major influence on the helicopter vertical response in hover since the vertical induced velocity mode often has a natural frequency near the regressing flap mode [18]. The identification model structure was therefore extended to include all of these dynamic effects in hover as well.

The overall model structure includes fuselage rigid body dynamics, second-order main rotor tip-path-plane flap and lead/lag dynamics, and collective dynamic induced velocity, main rotor/engine angular rate, engine torque, and engine fuel flow dynamics. The induced velocity, RPM, torque, and fuel flow dynamics largely decouple from the remainder of the model in forward flight.

Fuselage Equations

The fuselage dynamics are modeled with a modified version of the quasi-steady six degree of freedom aircraft stability derivative formulation. Derivatives due mostly to the high-frequency effects of main rotor flapping (e.g. L_p, M_q, etc...) are removed from the equations since these effects are modeled explicitly in the flapping equations. The standard quasi-steady control derivatives associated with inputs through the main rotor (e.g. L_{lat}, M_{lon}, etc...) are also removed since their effects now enter the model through the flapping equations as well.

Flapping Equations

The tip-path-plane flapping equations were derived through simplification of the linear equations of reference [19]. The equations were specialized to model frequencies near and above the flap regressing mode by eliminating vehicle velocity perturbation dependent terms from them. These effects are still modeled in the fuselage equations. The result is equations 1 through 3.

$$\ddot{a}_0 - \frac{M_\beta}{I_\beta}\dot{w} + C_{aero} = -\Omega^2\left(1 + e\frac{M_\beta}{I_\beta}\right)a_0 \tag{1}$$

$$\ddot{a}_1 + \dot{q} + 2\Omega\dot{b}_1 + A_{aero} = -\Omega^2 e\frac{M_\beta}{I_\beta}a_1 - 2\Omega\left(1 + e\frac{M_\beta}{I_\beta}\right)p \tag{2}$$

$$\ddot{b}_1 + \dot{p} - 2\Omega\dot{a}_1 + B_{aero} = -\Omega^2 e\frac{M\beta}{I\beta}b_1 + 2\Omega\left(1 + e\frac{M\beta}{I\beta}\right)q \tag{3}$$

The individual terms of the aerodynamic forces and moments (C_{aero}, A_{aero}, and B_{aero}) each depend on Lock number and include all of the main rotor control input terms. For example, the equation for A_{aero} with higher order terms removed is shown in equation 4.

$$\begin{aligned} A_{aero} = {} & \frac{\gamma\Omega}{2}\left[\frac{1}{4} - \frac{2}{3}\varepsilon\right]\dot{a}_1 - \mu\frac{\gamma\Omega^2}{2}\left[\frac{1}{3} - \frac{\varepsilon}{2}\right]a_0 \\ & + \delta_3\frac{\gamma\Omega^2}{2}\left[\frac{1}{4} - \frac{\varepsilon}{3} + \mu^2\left(\frac{1}{8} - \frac{\varepsilon}{4}\right)\right]a_1 \\ & + \frac{\gamma\Omega^2}{2}\left[\frac{1}{4} - \frac{2}{3}\varepsilon + \mu^2\left(\frac{1}{8} - \frac{\varepsilon}{4}\right)\right]b_1 \\ & + \frac{\gamma\Omega}{2}\left[\frac{1}{4} - \frac{\varepsilon}{3}\right]q \\ & - \frac{\gamma\Omega^2}{2}\left[\frac{1}{4} - \frac{\varepsilon}{3} + \mu^2\left(\frac{1}{8} - \frac{\varepsilon}{4}\right)\right]A_1 \end{aligned} \tag{4}$$

The parameters for which values are identified are Lock number, γ, pitch/flap coupling, δ_3, and the ratio M_β/I_β. The advance ratio, nominal rotor angular velocity, hinge offset, and rotor radius were fixed at their known physical values in the flapping equations. The resulting physical constraints between the terms of the flapping equations and these three free parameters were enforced in the identification.

Aerodynamic Phase Angle

Recent results from an identification study [11] using full-scale bearingless main rotor wind tunnel test data have been used here to modify the standard tip-path plane flapping equations to correctly capture the off-axis response. It is a much simpler approach than the one proposed by Rosen and is easily incorporated into the existing blade-element rotor theory in eqs 1-4.

As discussed in reference [11], the adjustment of the swashplate phase angle is equivalent to an azimuthal rotation in the fixed-frame rotor aerodynamics, or a "lag" in

the rotating frame (blade) aerodynamics. This is similar in effect to the Theodorsen function but larger in magnitude. The effective "aerodynamic phase lag", ψ_a, is defined in equation 5.

$$A'_{aero} = A_{aero}\cos\psi_a - B_{aero}\sin\psi_a$$
$$B'_{aero} = B_{aero}\cos\psi_a + A_{aero}\sin\psi_a \quad (5)$$

The variables A_{aero} and B_{aero} are the fixed-frame cosine and sine aerodynamic moment components for the conventional rotor formulation in Eqs 1-3. The variables A'_{aero} and B'_{aero} are the fixed-frame moments including the aerodynamic phase lag correction. The aerodynamic phase lag correction is included in the flapping dynamics identification by substituting A'_{aero} and B'_{aero} for A_{aero} and B_{aero} in equations 1-3. The aerodynamic phase lag, ψ_a, then becomes an additional parameter in the identification.

The corrected aerodynamic moments are also scaled according to equation 6 to ensure that the on-axis responses of the identified model are not significantly affected by the off-axis correction.

$$A''_{aero} = A'_{aero}\sec\psi_a$$
$$B''_{aero} = B'_{aero}\sec\psi_a \quad (6)$$

The lag in the rotating frame aerodynamics can be directly implemented in the body frame coning dynamics through the addition of a lagged aerodynamic force state to the model as given by

$$\tau\dot{C}'_{aero} + C'_{aero} = C_{aero} \quad (7)$$

where

$$\psi_a = \tau\Omega \quad (8)$$

Although the aerodynamic phase lag formulation is essentially comparable to swashplate tuning in the wind tunnel, this new approach also yields a correct prediction of cross-coupling for shaft-free flight simulation models. Analysis of an AH-64 helicopter has shown very close agreement between the results of Rosen's dynamic wake analysis, a similar implementation of the aerodynamic phase lag, and flight data. An advantage of the present approach is that the aerodynamic phase lag, ψ_a, can easily be identified for a range of flight conditions and incorporated into existing flight simulation models.

Cyclic Dynamic Inflow Model

The air mass dynamics are heavily coupled to the flapping dynamics in the hover flight condition, and, therefore, cannot be neglected in the present model. Previous identification studies [24] have shown, however, that excessive parameter correlation makes it very difficult to identify inflow dynamics parameters even when rotor blade motion measurements are available. An alternative, which has been shown to be viable in two previous identification studies [9, 24], is to absorb the effects of the first harmonic inflow into the flapping equations through the use of the reduced Lock number [25] of Eq. 9.

$$\gamma^* = \frac{\gamma}{1+\frac{a\sigma}{16\bar{v}_0}} \quad (9)$$

The reduced Lock number was therefore used in the flapping equations, while the actual Lock number was identified in the coning equation. The reduced Lock number was constrained to the actual Lock number in the identification according to Eq 9.

Lead-Lag Dynamics

Simple identification model structures are not available for the lead-lag dynamics in terms of the physical rotor parameters. As discussed in reference [22], the dominant effect of the lead-lag dynamics on the control system design problem is the addition of a second-order dipole appended to the roll-rate response to lateral stick. Another dipole with the same denominator eigenvalues was appended to the pitch response. This approach has been satisfactory in the previous identification of the BO-105 and UH-60 dynamics [23, 9].

Additional Dynamics

The vertical inflow, vertical velocity, and rpm equations of [9] were rederived to include explicit dependence on coning. The various terms of the coning, inflow, and vertical velocity equations, as functions of the aircraft physical parameters, agree with the results given in Ref. [18], as do the rotor RPM equation. The coning equation was also extended to include the effects of rpm and yaw rate variations.

Identification Method

The frequency-response-error method of CIFER® [23] was used to identify the models presented in this paper. First, CIFER® is used to identify high quality, broad-band frequency responses from the flight test data. Then, parameter values in the state-space representation of the system dynamics are determined by CIFER® through minimization of the weighted fit errors between the model and frequency responses.

The model structure is reduced to a minimum set of parameters by sequentially dropping the relatively insignificant parameters and reconverging the remaining model parameters to a best fit of the data until the overall cost function increases significantly. The choice of which parameter to drop is based on calculations of parameter insensitivities, Cramer-Rao bounds, and multiple parameter correlations each time the model is reconverged. Insensitive parameters are removed until a minimum number of parameters with insensitivity values exceeding a target value of 10% remain. Excessively-correlated parameters are then removed until a minimum number of parameters with Cramer-Rao percents greater than a target value of 20% remain. This approach has been found to be very reliable in model structure reduction, validating the relevance of the chosen accuracy metrics.

The final, minimally-parameterized model is checked for robustness by driving it with flight-measured control inputs of a different character than those used in the identification, and comparing the model responses to those measured in flight. The reader is referred to reference [23] for additional background on CIFER®.

Flight Test Results

Data Collection

A flight test program was initiated to collect flight test data suitable for open-loop identification and verification using the RASCAL UH-60 helicopter. Tests were conducted in hover and 80 kts forward flight under very calm wind conditions at the Ames flight test facility located at Crows Landing, CA in September, 1992. The takeoff gross weight was approximately 14,350 lb. and the c.g. was at station 360. for all flights.

Additional engine response flight test data from the Airloads UH-60 [26] were used to supplement the RASCAL flight test data in order to extend the hover model to include coupled body/rotor/engine dynamics. Merging these two data bases was deemed reasonable because the engine response dynamics are not highly airframe specific. An advantage of the frequency response identification process is the flexibility to use data from non-concurrent flight test records.

Frequency sweeps [27], 2-3-1-1 multisteps* , and doublets were manually input into each pilot control with the Stability Augmentation System (SAS) and Flight Path Stabilization (FPS) system disengaged. The pilot was asked to minimize the use of off-axis inputs during the maneuvers to prevent correlation between controls. An effective piloting technique is to maintain the trim condition and stabilize the aircraft using pulse type inputs in the off-axis controls. Each maneuver was repeated several times to ensure sufficient data. The stabilator was fixed at the hover trim value of 40 degrees trailing-edge-down during hover and four degrees trailing-edge-down at 80 kts.

Good low frequency identification was achieved by sufficiently, but not excessively exciting the low frequency dynamics during the frequency sweeps with the SAS and FPS off. This means that attitude and position perturbations were noticeable to the pilot, but were not large enough to cause difficulty in maintaining stability at the trim condition. Flying with the stability augmentation disengaged improves the quality of the low frequency identification by preventing control correlations caused by feedback. Previous identification of UH-60 low frequency characteristics, particularly in the longitudinal axis, has been limited by availability of SAS-ON data only [26]. SAS/FPS-OFF low frequency inputs were achieved by modulating the low frequency amplitude of the frequency sweep to prevent large attitude excursions and superimposing pulse type inputs to prevent excursions away from the trim condition. This type of modulation keeps the response in the linear region, helps to maintain trim, eases the task of stabilization, and actually serves to enrich the frequency content of the input. A perfect swept sine wave is neither necessary nor desired.

Instrumentation and Data Consistency

Control positions were measured with string pots attached to the mechanical control system linkages. Response variables were measured by a Litton LN-93 Inertial Navigation Unit (INU) mounted on the cabin floor. The INU calculates body attitudes, angular rates, specific forces, and inertial velocities from ring laser gyro and accelerometer triads. These data are Kalman-filtered and output to a digital data bus at 256 Hz with minimal phase lag. The control position signals were digitized and merged with the digital output from the LN-93. Anti-alias filtering of the control positions was not necessary because the bandwidth of the potentiometers is significantly lower than the sample rate [28]. Digital output from a GEC Helicopter Air Data Sensor (HADS) system was also recorded onboard. LASER tracking data were recorded during hover by the ground station and merged with the on-board data in a post processing step.

Kinematic consistency of the response variables was checked with the optimal state estimation program SMACK [29] using the procedure outlined in reference [30]. This was done primarily to correct the measurements to the c.g., remove small drifts from the INU calculated velocities, and detect and remove disturbances from the air data. Excellent on-board data consistency and compatibility with the LASER derived inertial velocities was verified.

Frequency Response Identification

Frequency responses were calculated from the frequency sweep inputs for the angular rate, linear velocity, and linear acceleration responses of the helicopter to each of the four pilot controls. Excellent excitation of the aircraft dynamics in the frequency range of 0.1 to 20 rad/sec was achieved. As a result, 29 of the 36 possible frequency responses were included in the stability derivative identification for hover and 30 out of 36 for 80 kts.

Pitch and roll rate frequency responses identified with CIFER® from the flight test data are shown in Figures 3 and 4 for the hover and 80 kts flight conditions respectively. The coherence function indicates the extent to which the output is linearly related to the input. Factors which degrade the coherence function from a maximum value of one are: lack of input excitation, lack of aircraft response, process noise such as gusts, and significant non-linearities in the dynamics. Coherence values of 0.6 and above are considered acceptable. The coherence function is used as a weighting function by CIFER® in minimizing frequency response errors to determine the values of the parameters in the state space model.

Referring to Figure 3, it is evident that excellent identification of the on-axis responses has been achieved in the frequency range of 0.5 to 20 rad/sec for the hover flight

* 2-3-1-1 Multisteps are a series of step type inputs alternating in direction of the input and with relative time durations of two units, three units, one unit, and one unit. The steps are performed sequentially, to form one time record, starting and ending at the trim contol position.

condition. The coherence of the off-axis response is not as good, but these data definitely supply sufficient information about the coupled response to be used in the stability derivative identification. The p/δ_{lon} response is better identified than the q/δ_{lat} response because there is more roll rate response due to a much smaller aircraft roll moment of inertia. The effects of rotor flapping can be seen in the downward break in the hover q/δ_{lon} and p/δ_{lat} magnitude curves above eight rad/sec, emphasizing the importance of these dynamics in the frequency range for flight control. The lead-lag mode dominates both the magnitude and phase curves of the on-axis frequency responses above 13 rad/sec.

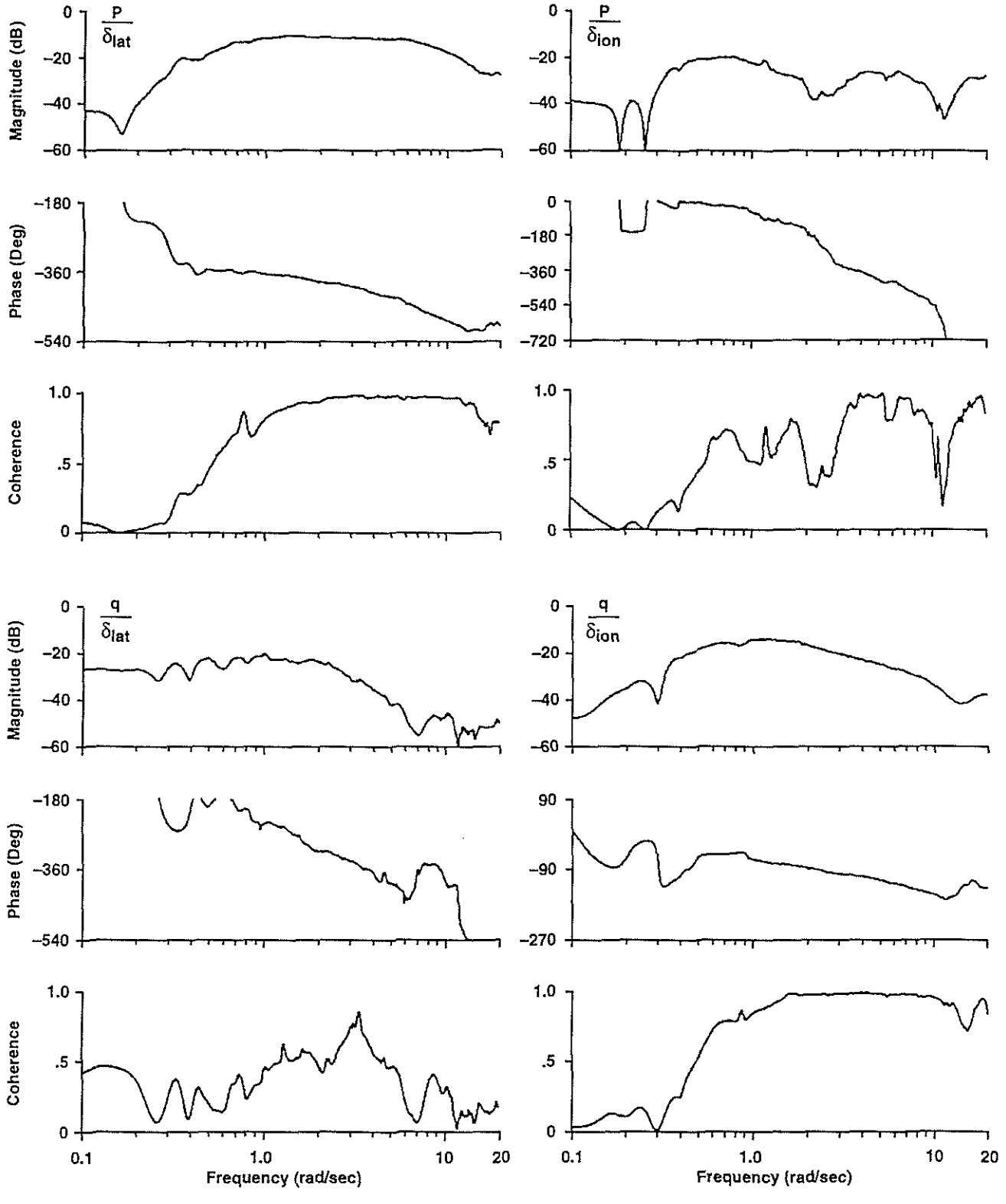

Figure 3. CIFER®-Identified Frequency Responses for UH-60 in Hover

Referring to Figure 4, the forward flight results are generally similar to those in hover. A significant difference is that the quality of the frequency responses above 15 rad/sec is not as good. This is probably due to a lack of high frequency inputs since these sweeps were flown by a different pilot.

However, the low-frequency identification results are of higher quality than the hover results. It is generally easier to achieve better low-frequency identification in forward flight because it is easier to maintain trim while conducting the frequency sweep.

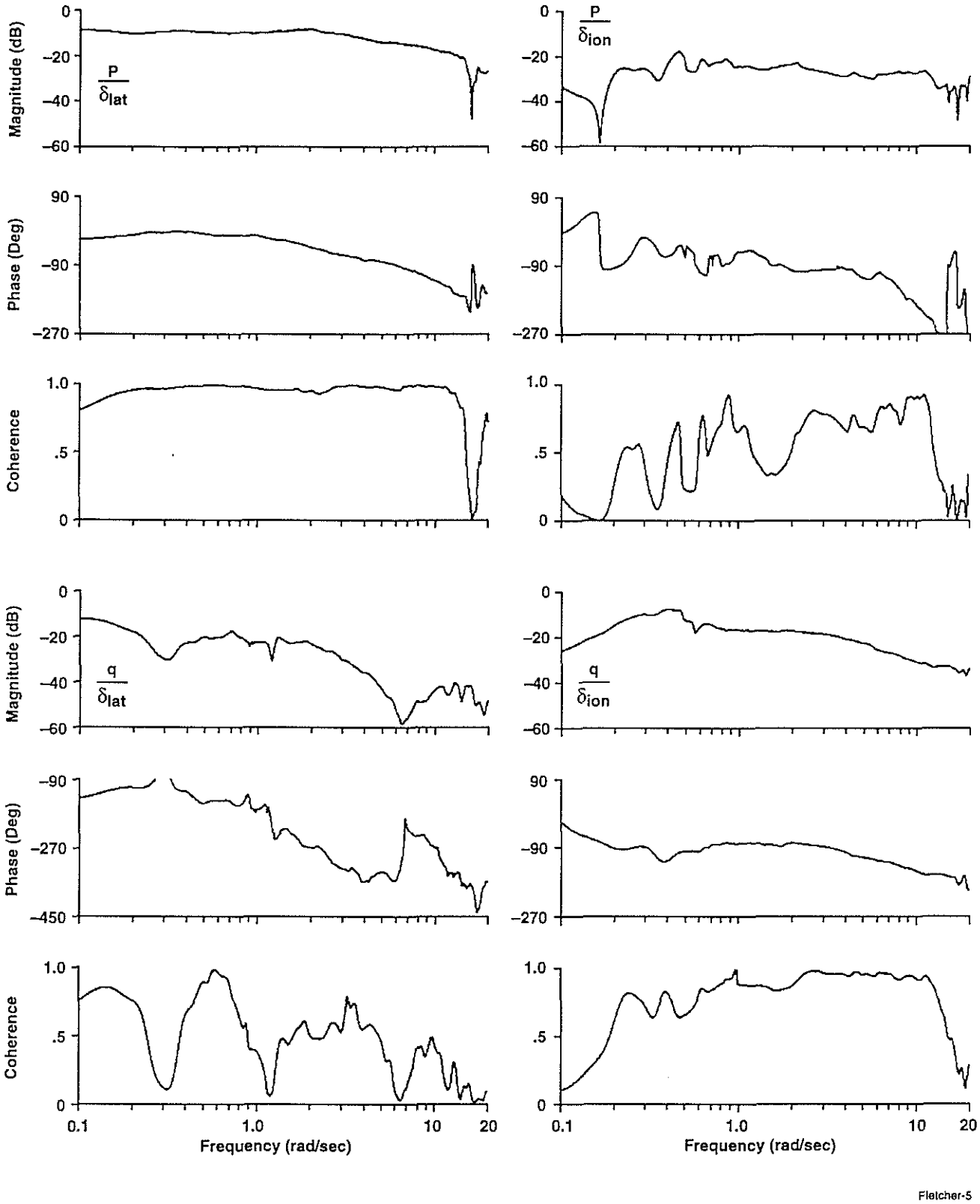

Figure 4. CIFER®-Identified Frequency Responses for UH-60 in 80 Knots Forward Flight

Hover Identification Results

The overall identification model structure, excluding lead-lag was fit to 29 RASCAL hover-identified frequency responses and the RPM and torque frequency responses from the Airloads database. The pitch and roll angular rate responses were fit up to 12 rad/sec, at which point the first effects of the lead-lag mode are seen. The hover model parameters were then fixed at their final values and the lead-lag dynamic parameters which optimized the fits of the q/δ_{lon} and p/δ_{lat} frequency responses up to 20 rad/sec were identified.

The equivalent time delays on the control inputs were fixed at a value representative of the hydraulic system delay. Modeling additional delay was not necessary since all of the significant sources of phase lag below 20 rad/sec are explicitly modeled. A value of 0.026 sec was identified from the frequency response of the lateral primary servo which agrees very well with the value of 0.024 identified by Ballin [26] for the Airloads UH-60.

The fuselage parameters of the model of reference [9] were used for startup of the hover model identification. The rotor parameters were also set at theoretical values for startup. The model structure was reduced as previously described to achieve a minimally parameterized hover model.

The identified rotor flapping parameters are compared with theoretical values in Table 1. The identified Lock number and blade mass moment ratio are reasonably close to theoretical results. A stable value of pitch-flap coupling is identified which contributes significantly to the measured response. The aerodynamic phase lag is large ($\psi_a = 39$ deg) and indicates that a significant correction to the classical flapping equations is required to match the off-axis response in hover.

Table 1: Comparison of theoretical and identified parameters

Parameter	Identified Value	Theoretical Value
γ	8.62	8.06
M_β/I_β	0.0321	0.0573
δ_3	7.84 deg	0.0
ψ_a	38.8 deg	N.A.

Frequency Response Results

Figure 5 compares the on-axis roll rate frequency response to lateral cyclic of the identified model, linearized versions of BE models A and B [4], [3], and the flight test data. The identified model fit is good up to 20 rad/sec, well into the frequency range dominated by the regressing flap and lead-lag modes. The lead-lag mode is quite evident in the 15 to 20 rad/sec frequency range and is matched well by the identified model. The linearized blade element models are both deficient in capturing the frequency of the lead-lag mode.

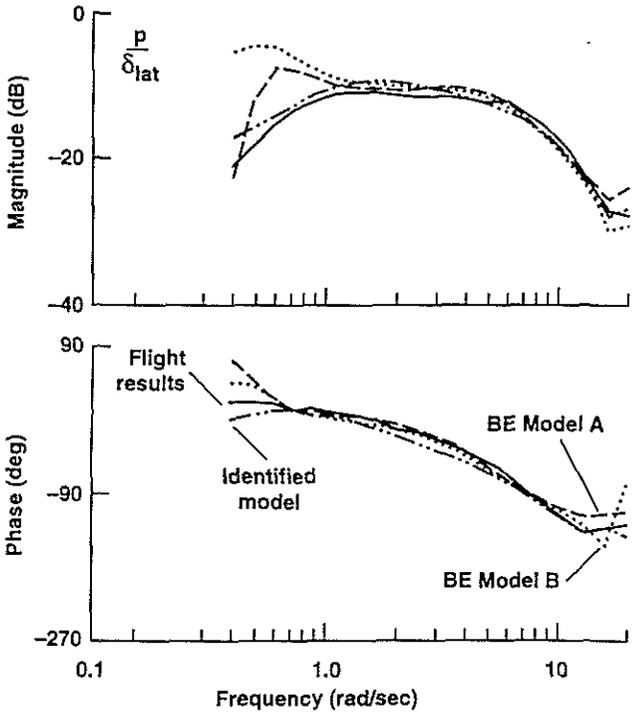

Figure 5. Hover comparison of p/δ_{lat} frequency responses

Figure 6 shows a significant improvement in the fit of the coupled response over that of blade element models A and B. The simulation models have considerable phase error in this response, which is typical of current component type rotorcraft simulation models. The identified model accurately describes the coupled response well up to six rad/sec. Identification above six rad/sec is not possible due to low coherence.

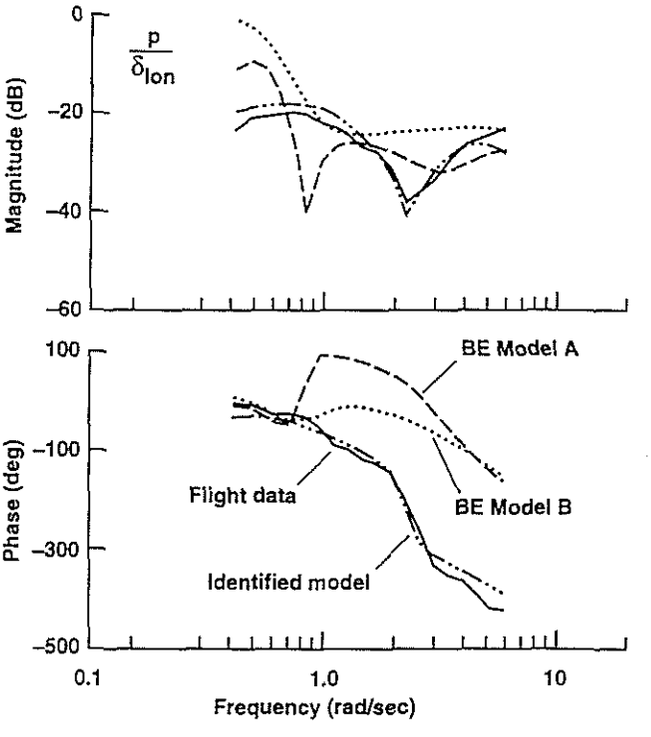

Figure 6. Hover Comparison of p/δ_{lon} frequency responses

Figures 7 and 8 show that the identified hover model captures the important yaw/heave coupling characteristics of the UH-60 in hover. Both the identified model and blade element model B include RPM and engine/governor dynamics which are clearly needed to match the r/δ_{col} response. However, only the flight identified model matches the a_z/δ_{ped} data in Figure 8. This indicates that some other phenomena may be modeled in the identification, which is not included in either of the simulation models.

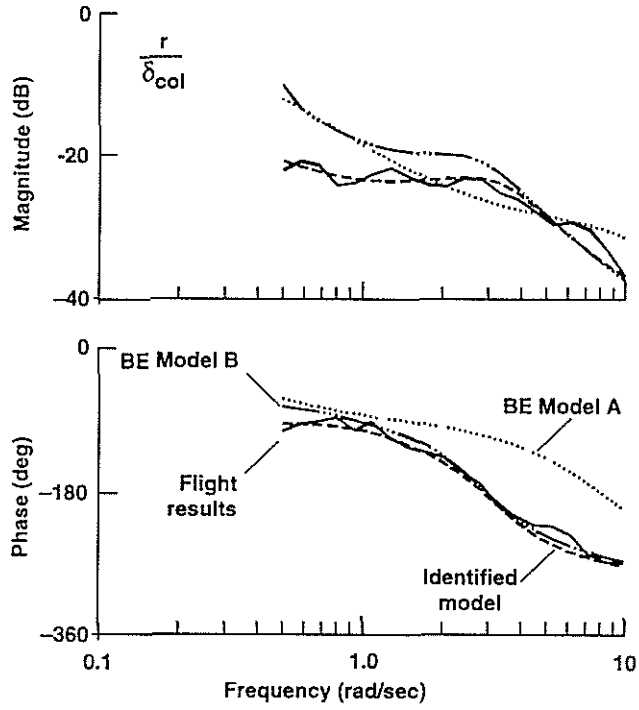

Figure 7. Hover Comparison of r/δ_{col} frequency responses.

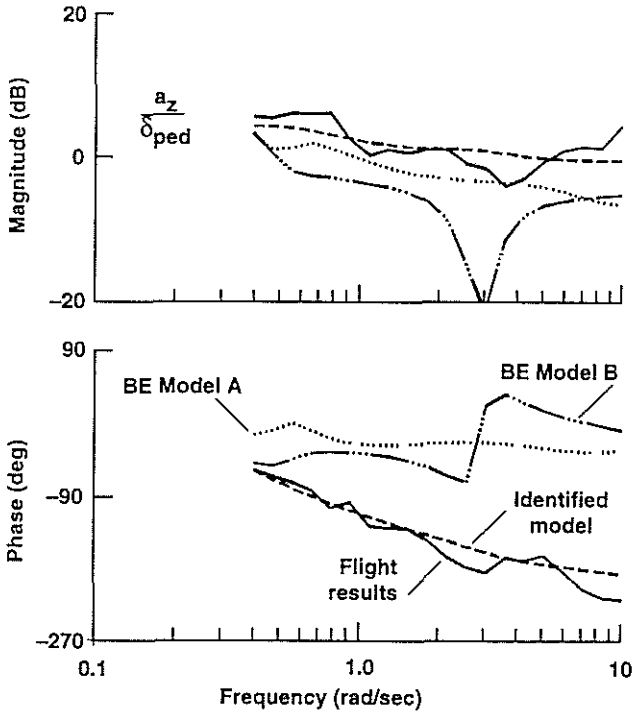

Figure 8. Hover comparison of a_z/δ_{ped} frequency responses.

Effect of Aerodynamic Phase Lag

Figure 9 shows the effect of the aerodynamic phase lag on the identified model. The figure compares the off-axis roll rate response to longitudinal cyclic input for the identified model with aerodynamic phase lag of $\psi_a = 39$ deg and a baseline case of $\psi_a = 0$ deg to the flight-identified results. Including the aerodynamic phase lag is seen to greatly improve the correlation of the off-axis response. The baseline case magnitude curve looks very similar to the BE model A p/δ_{lon} response and the phase curve is also similar at high frequency. This is not surprising since the BE model does not contain the aerodynamic moment phasing effect.

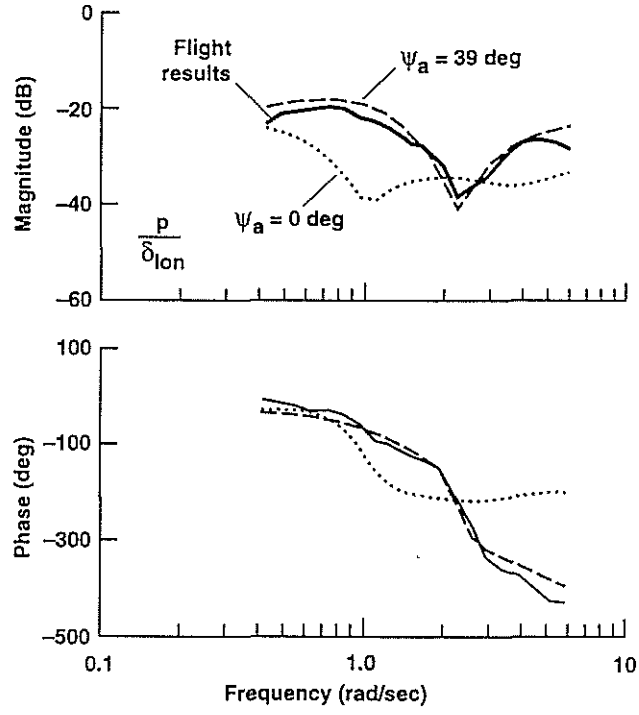

Figure 9. Effect of Aerodynamic Phase lag on Identification

Hover Time Domain Verification

The identified model was checked for robustness by driving it with flight measured control inputs different in character than those used in the identification process. Figure 10 compares the model time responses from a pitch doublet input to those measured in flight. The on and off-axis responses of the model closely track the measured aircraft response in the time domain and validates the identification model.

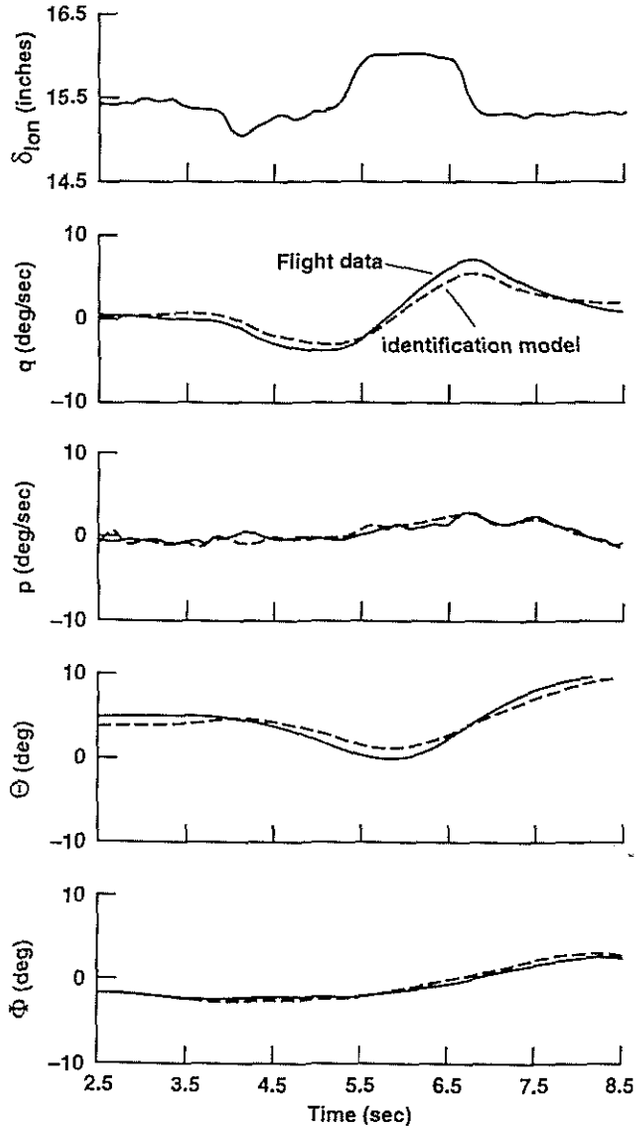

Figure 10. Time Domain Verification of Hover Model

80 Knots Identification Results

The identification model structure was simplified somewhat for the 80 Kts identification. The collective dynamic induced velocity, rotor angular velocity, and engine/governor dynamics were removed, reflecting the reduced importance of these dynamics in the forward flight condition.

The remaining structure, excluding lead-lag dynamics was fit to 30 RASCAL 80 Knots-identified frequency responses. The pitch and roll angular rate responses were fit up to 12 rad/sec, at which point the first effects of the lead-lag mode are seen. The model parameters were then fixed at their final values and the lead-lag dynamic parameters, which optimized the fits of the q/δ_{lon} and p/δ_{lat} frequency responses up to 20 rad/sec, were identified.

Startup values for the rigid body parameters were obtained from a linearized version of blade element model A at 80 kts, and startup values for the flapping parameters were obtained from the hover identification. The Lock number, γ, and blade mass moment ratio, M_β/I_β, were fixed at the hover identified values for the 80 Kts identification.

The important rotor flapping parameters identified for 80 Kts are compared with the values identified for hover in Table 2. The Lock number and blade inertia ratio, M_β/I_β, were fixed at the hover identified values. The pitch/flap coupling and aerodynamic phase lag were well identified according to the Cramer-Rao bounds and parameter sensitivity calculations. The value of pitch flap coupling is similar to that identified in hover, as expected.

A much smaller value of the aerodynamic phase lag is identified for 80 kts than for hover. Since the exact mechanism of this effect is not known, it is not possible to comment with certainty on the adequacy of this result. However, it is reasonable that the effect of the dynamic wake, like the effect of inflow, on the flapping dynamics is diminished with increasing advance ratio. Simulation studies of other helicopters have yielded similar trends in the value of the aerodynamic phase lag required for a best fit of flight data.

Table 2. Comparison of identified rotor parameters

Parameter	Hover Identified Value	80 Kts Identified Value
γ	8.62	8.62
M_β/I_β	0.0321	0.0321
δ_3	7.84 deg	9.86 deg
ψ_a	38.8 deg	15.1 deg

Frequency Response Comparisons

Frequency responses of the identified model are compared with those of BE model A and flight test data at the 80 kts flight condition in figure 11 through 14. The identified model fits both the on-axis and coupled responses much better than does the linearized simulation model. Of particular interest is the mismatch between BE model A and the flight test data below 3 rad/sec. Although this frequency range is not as critical for the FCS design application, the errors are very significant. Phase errors between the identified and BE models in the q/δ_{lat} frequency response approach 180 degrees near four rad/sec indicating a sign error discrepancy. This result is similar to that seen in the hover off-axis response case.

Discrepancies between the BE model A and flight are significant for the yaw and heave coupled responses at 80 Knots. The mismatch in the r/δ_{col} response is greater than in hover, while the a_z/δ_{ped} response mismatch is smaller. The excellent fit of the identified model without drivetrain dynamics indicates that this is not the source of the problem for BE model A.

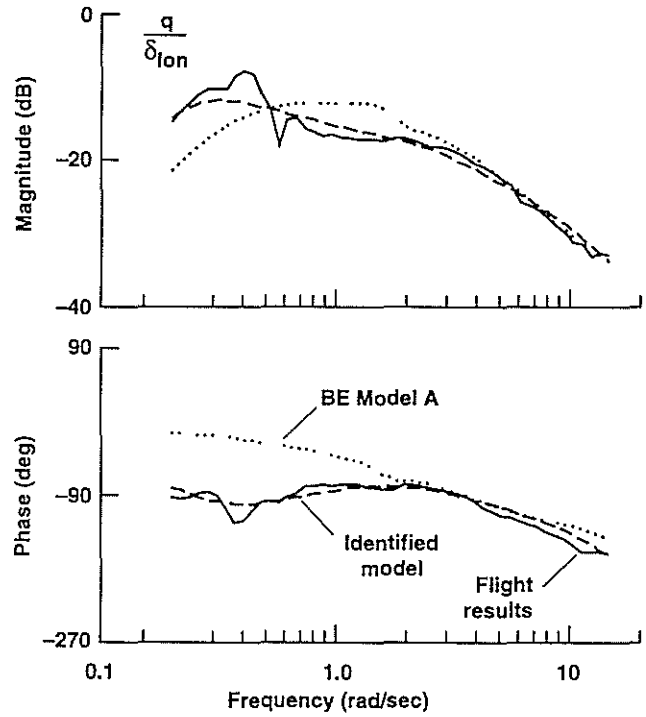

Figure 11. 80 Knots Comparison of q/δ_{lon} frequency responses.

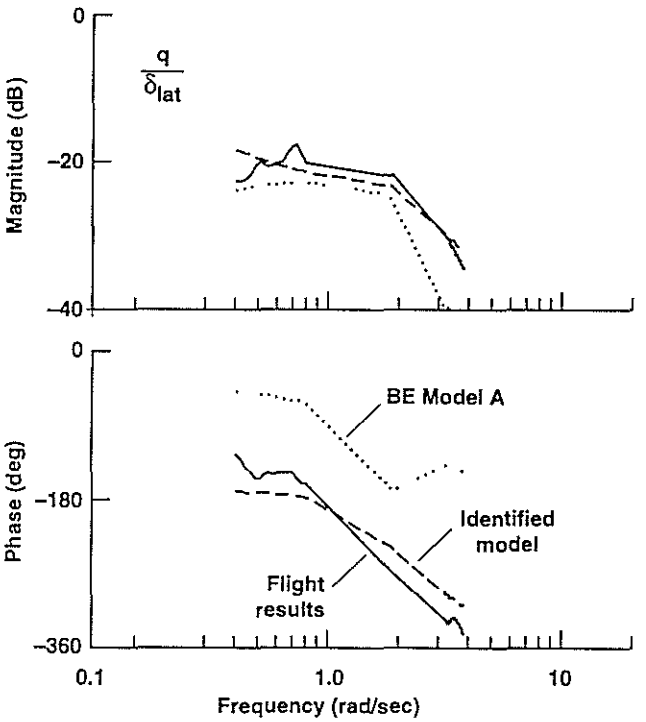

Figure 12. 80 Knots Comparison of q/δ_{lat} frequency responses.

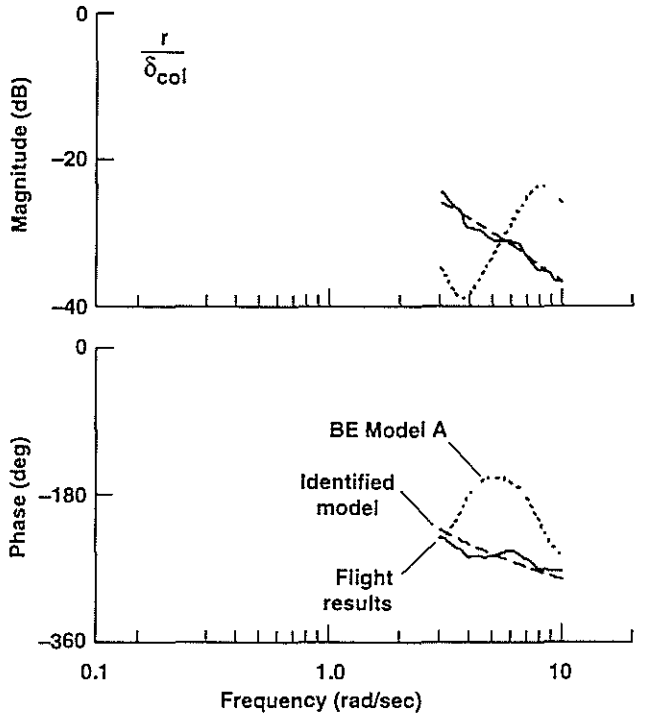

Figure 13. 80 Kts Comparison of r/δ_{col} frequency responses.

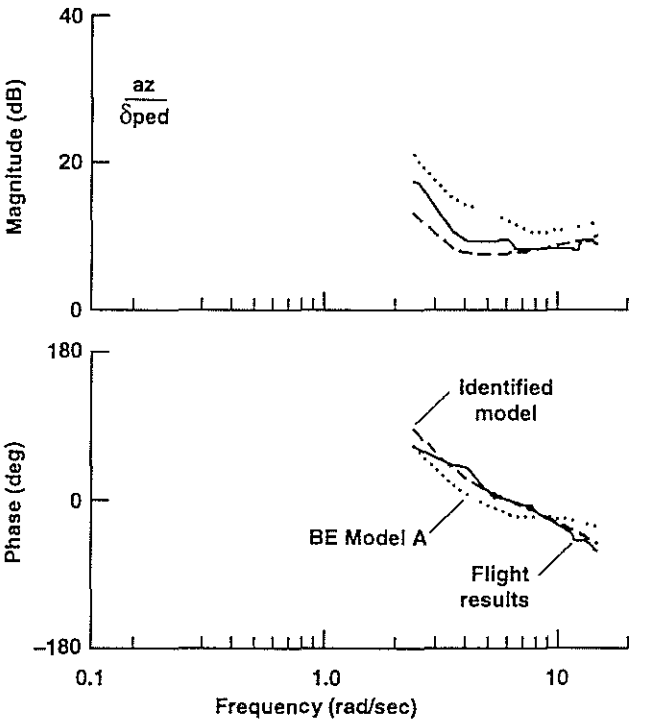

Figure 14. 80 Kts Comparison of a_z/δ_{ped} frequency responses.

80 Knots Time Domain Verification

The identified model at 80 Knots was checked for robustness by driving it with flight measured control inputs different in character than those used in the identification process. Figure 15 compares the model time responses from a pitch doublet input to those measured in flight. The on and off-axis responses of the model closely track the measured aircraft response in the time domain and validates the identification model. The fits are not as good as the hover case, but the responses are also much larger. This could be an indication of the limit of response amplitudes for which the small perturbation, linear analysis is valid.

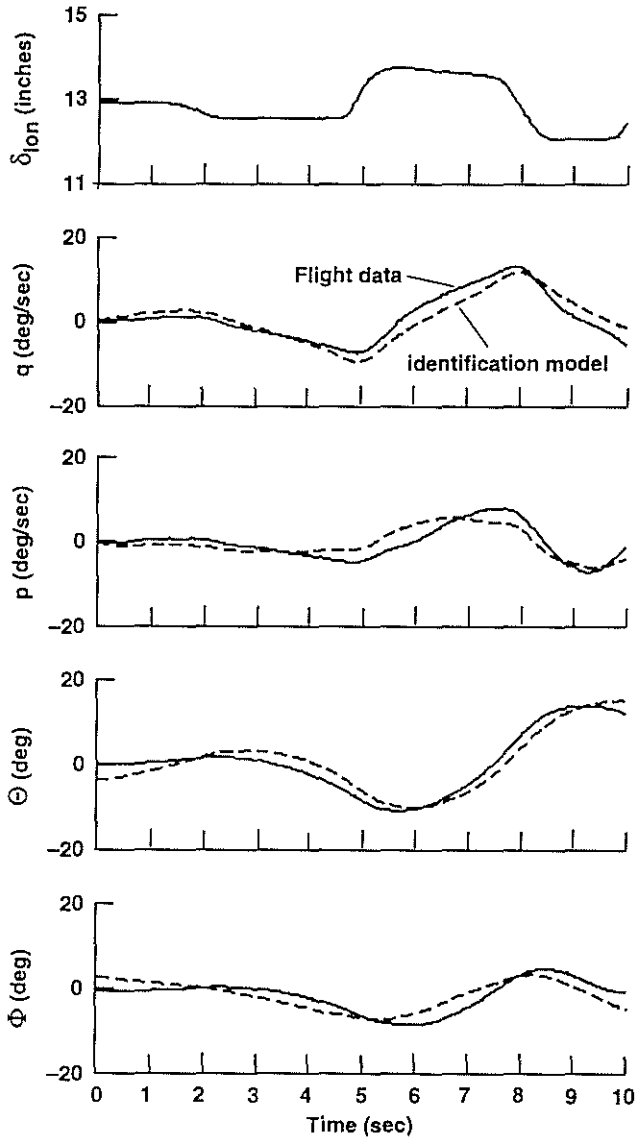

Figure 15. Time Domain Verification of 80 Knots Model

Summary and Conclusions

A model structure applicable to the identification of linear models of the UH-60 in hover and forward flight has been developed. Fuselage linear and angular degrees of freedom, main rotor flap and lead-lag, collective induced velocity, main rotor/engine RPM, and engine/governor dynamics are included in the general linear model structure formulation. The new model structure:

(1) is appropriate for identification of models for use in the design of high bandwidth control laws for the UH-60 at hover and 80 kts forward flight,

(2) introduces the aerodynamic phase lag parameter into the flapping dynamics, allowing identification of models which correctly predict the off-axis response without relaxing physical constraints in the equations of motion, and

(3) is not overparameterized when flapping data are not available for use in the identification.

It was used to identify linear models of the UH-60 flight dynamics at hover and 80 kts forward flight which:

(1) adequately fit the flight test data and accurately predict the vehicle response to pilot inputs in the frequency range of 0.3 to 20 rad/sec,

(2) predict the on-axis responses of the helicopter with at least equal fidelity and the off-axis angular responses to cyclic controls with improved fidelity when compared with two blade element simulation models of the UH-60, and

(3) predict the yaw-heave coupling of the helicopter with improved fidelity compared to the blade element models.

References

[1] Tischler, M.B., "Digital Control of Highly Augmented Combat Rotorcraft," NASA TM-88346, USAAVSCOM Technical Report 87-A-5, May, 1987.

[2] Curtiss, H.C., Jr., "On the Calculation of the Response of Helicopters to Control Inputs," 18th European Rotorcraft Forum, Avignon, France, September, 1992.

[3] Takahashi, M.D., "A Flight-Dynamic Helicopter Mathematical Model with Single Flap-Lag-Torsion Main Rotor," NASA TM 102267, USAAVSCOM TM 90-A-004, February, 1990.

[4] Kim, F.D., "Analysis of Propulsion System Dynamics in the Validation of a High-Order State Space Model of the UH-60," AIAA/AHS Flight Simulation Technologies Conference, Hilton Head, SC, August, 1992, AIAA-92-4150-CP.

[5] Peters, D.A., and HaQuang, N., "Dynamic Induced velocity for Practical Applications," *Journal of the American Helicopter Society*, Vol. , No. , pp. 64-68, October, 1988.

[6] Takahashi, M.D., Fletcher, J.W., and Tischler, M.B., "Development of a Model Following Control Law for Inflight Simulation Using Analytical and Identified Models," 51st Annual Forum of the American Helicopter Society, Fort Worth, TX, May, 1995.

[7] Mansur, M.H., "Development and Validation of a Blade-Element Mathematical Model for the AH-64 Apache Helicopter," USAATCOM Technical Memorandum 108863, April, 1995.

[8] 8 FMP WG-18, "Rotorcraft System Identification," 8 Advisory Report 280, 8-AR-280, 1991.

[9] Fletcher, J.W. ,"Identification of UH-60 Stability Derivative Models in Hover from Flight Test Data," *Journal of the American Helicopter Society*, Vol. 40, No. 1, pp. 32-46, January, 1995.

[10] Rosen, A. and Isser, A., "A New Model of Rotor Dynamics During Pitch and Roll of a Hovering Helicopter." 50th American Helicopter Society Annual Forum, Washington, DC, May 11-13, 1994.

[11] Tischler, M.B., Driscoll, J.T., Cauffman, M.G. and Freedman, C.J., "Study of Bearingless Main Rotor Dynamics from Frequency-Response Wind Tunnel Test Data, " paper presented at the AHS Aeromechanics Specialists Conference, San Francisco, CA, January 19-21, 1994.

[12] Aiken, E., Jacobsen, R., Eshow, M., Hindson, W., and Doane, D., "Preliminary Design Features of the RASCAL - A NASA/Army Rotorcraft In-Flight Simulator," AIAA-92-4175, August, 1992.

[13] Chen, R.T.N and Hindson, W.S., "Influence of high-order dynamics on helicopter control system bandwidth," *AIAA Journal of Guidance, Control, and Dynamics*, Vol. 9, No. 2, pages 190-197, 1986.

[14]Takahashi, M.D., "Rotor-State Feedback in the Design of Flight-Control Laws for a Hovering Helicopter," *Journal of the American. Helicopter. Society*, Vol. 39, No. 1. January 1994.

[15] Hilbert, K.B., Lebacqz, J.V., and Hindson, W.S., "Flight Investigation of a Multivariable Model-Following Control System for Rotorcraft," AIAA paper 86-9779, AIAA 3rd Flight Test Conference, Las Vegas, NV, April 2-4, 1986

[16] Kaletka, J. and von Grünhagen, W., "Identification of Mathematical Derivative Models for the Design of a Model Following Control System," 45th Annual Forum of the American Helicopter Society, Boston, MA, May, 1989.

[17] Chen, R.T.N., "An Exploratory Investigation of the Flight Dynamic Effects of Rotor RPM Variations and Rotor State Feedbacks in Hover," 18th European Rotorcraft Forum, Avignon, France, September, 1992.

[18] Chen, R.T.N. and Hindson, W.S., "Influence of Dynamic Induced velocity on the Helicopter Vertical Response." NASA TM-88327, June, 1986.

[19] Chen, R.T.N., "A Simplified Rotor System Mathematical Model for Piloted Flight Dynamics Simulation," NASA TM-78575, May, 1979.

[22] Tischer, M.B., "System Identification Requirements for High-Bandwidth Rotorcraft Flight Control System Design," *Journal of Guidance, Control, and Dynamics*, vol 13, no 5, 1990, pp 835-841.

[23] Tischler, M.B., and Cauffman, M.G., "Frequency-Response Method for Rotorcraft System Identification: Flight Applications to BO 105 Coupled Rotor/Fuselage Dynamics," *Journal of the American Helicopter Society*, Vol 37, No 3, pp. 3-17, July, 1992.

[24] Harding, J.W.,"Frequency Domain Identification of Coupled Rotor/Body Models of the AH-64," 48th Annual Forum of the American Helicopter Society, Washington, D.C., June, 1992.

[25] Curtiss, H.C., Jr.,"Stability and Control Modeling," *Vertica*, Vol. 12, No. 4, 1988.

[26] Ballin, M.G. and Dalang-Secretan, M.A., "Validation of the Dynamic Response of a Blade-Element UH-60 Simulation Model in Hovering Flight," 46th Annual Forum of the American Helicopter Society, Washington, D.C., May, 1990.

[27] Tischler, Fletcher, J.W., Diekman, V.L., Williams, R.A., and Cason, R.W., "Demonstration of Frequency-Sweep Testing Technique Using a Bell 214-ST Helicopter," NASA TM 89422, USAAVSCOM TM 87-A-1, April, 1987.

[28] Holland, R.,"Digital Processing of Flight Test Data of a Helicopter without Using Anti-Aliasing Filters," ESA translation from DFVLR-Mitt. 87-12, ESA-TT-1094, 1987.

[29] Bach, R.E., Jr., "State Estimation Applications in Aircraft Flight-Data Analysis: A User's Manual for SMACK," NASA RP 1252, March, 1991.

[30] Fletcher, J.W.,"Obtaining Consistent Models of Helicopter Flight-Data Measurement Errors Using Kinematic -Compatibility and State-Reconstruction Methods," 46th Annual Forum of the American Helicopter Society, Washington, D.C., May, 1990.